Are matrix isolated species really "isolated"? Infrared spectroscopic and theoretical studies of noble gas-transition metal oxide complexes

ZHAO YanYing & ZHOU MingFei[*]

Department of Chemistry, Shanghai Key Laboratory of Molecular Catalysts and Innovative Materials,
Advanced Materials Laboratory, Fudan University, Shanghai 200433, China

In this review, we summarize our recent results on matrix isolation infrared spectroscopic studies and theoretical investigations of noble gas–transition metal oxide complexes. The results show that some transition metal oxide species trapped in solid noble gas matrices are chemically coordinated by one or multiple noble gas atoms forming noble gas complexes and, hence, cannot be regarded as isolated species. Noble gas coordination alters the vibrational frequencies as well as the geometric and electronic structures of transition metal oxide species trapped in solid noble gas matrixes. The interactions between noble gas atoms and transition metal oxides involve ion-induced dipole interactions as well as chemical bonding interactions. Periodic trends in the bonding in these noble gas-transition metal complexes are discussed.

noble gas complexes, transition metal oxides, matrix isolation, infrared spectroscopy

1 Introduction

Since the first report in 1954 by Pimentel and co-workers [1], matrix isolation has proven to be one of the most important methods for trapping and isolating free radicals and other reactive intermediates for spectroscopic studies [2–5]. Noble gases, such as Ne and Ar, are commonly used as matrices, which are sufficiently rigid to effectively isolate the reactive species at low temperatures (4–10 K). Due to the remarkable stability of the closed-shell ground state electronic configuration, noble gas atoms are generally considered to be chemically inert. Therefore, it is usually assumed that the noble gas matrix that confines the free radicals and reactive intermediates is electronically innocent—that is, the species trapped in the solid matrix are normally regarded as isolated "gas phase" molecules. In general, the molecular properties measured in solid noble gas matrices are only slightly different from those measured in the gas phase. A comparison of the ground state vibrational fundamentals of several hundreds of molecules observed in the gas phase and in noble gas matrices has shown that matrix shifts of most diatomic molecules isolated in solid argon are less than 2%, and shifts for molecules trapped in solid neon are even smaller [6, 7]. Considerable differences between the values of measured vibrational fundamentals in the gas phase and in different noble gas matrices have also been reported in many cases, however, which are assumed to be caused by "matrix effect".

However, noble gas atoms are not completely chemically inert. Since the report [7, 8] of the first stable xenon-containing compound, $XePtF_6$, a large number of chemically bound complexes containing heavier noble gas atoms have been prepared [9, 10]. Recent investigations have shown that even a light noble gas, argon, is able to form the chemically bound compound HArF in solid argon [11]. It has also been found that noble gas atoms are able to coordinate to metal centers and form noble gas–metal complexes. The group

*Corresponding author (email: mfzhou@fudan.edu.cn)

VIB pentacarbonyls are able to coordinate one noble gas atom to form the M(CO)$_5$(Ng) complexes (M = Cr, Mo, W; Ng = Ar, Kr, Xe) in solid noble gas matrices or in liquid Xe [12–16]. The M–Xe binding energies of these M(CO)$_5$(Xe) complexes have been determined to be 9.0 ± 0.9 (Cr), 8.0 ± 1.0 (Mo), and 8.2 ± 1.0 kcal/mol (W) by measuring the temperature dependence of the dissociation rate constant in the gas phase [17]. The Fe(CO)$_4$ radical reacts with Xe to form the Fe(CO)$_4$(Xe) complex in supercritical liquid Xe solution [18]. Besides the above-mentioned noble gas–transition metal carbonyl complexes, a number of noble gas–organometallic complexes such as (η^5-C$_5$H$_5$)Mn(CO)$_2$-(Xe), (η^5-C$_5$H$_5$)M(CO)$_3$(Xe) (M = Nb, Ta), Rh(CO)(PMe$_3$)$_2$-(Ng) (Ng = Kr, Xe), (η^5-C$_5$H$_5$)Rh(CO)(Ng) (Ng = Xe and Kr), Cp*Rh(CO)(Ng) (Cp* = η^5-C$_5$Me$_5$; Ng = Xe and Kr), and Re(η^5-C$_5$H$_5$)(CO)$_2$(Xe) have also been characterized in solution at room temperature [19–27]. Strong noble gas–transition metal bonding has been observed in some noble metal systems [28–38]. The [AuXe$_4$]$^{2+}$[Sb$_2$F$_{11}^-$]$_2$ salt provides the first crystallographic evidence of a transition metal–noble gas bond with a binding energy of approximately 200 kJ/mol with respect to Au^{2+} and Xe [28]. The linear noble gas–noble metal mono-halide complexes (Ng)MX (Ng = Ar, Kr, Xe; M = Cu, Ag, Au; X = F, Cl, Br) have also been shown to involve strong noble gas–noble metal interactions with very short and rigid M–Ng bonds [32–38].

The above-mentioned examples suggest that transition metal-containing compounds trapped in solid noble gas matrixes may be chemically coordinated by noble gas atoms, and cannot be regarded as isolated species. Noble gas coordination may change the geometric and electronic structures and reactivity of the species trapped in solid matrixes. Recent investigations have provided evidence that CUO molecules (prepared by reaction of laser-ablated uranium atoms with CO) trapped in solid noble gas matrices are coordinated by multiple noble gas atoms with direct bonding interactions between the uranium center and noble gas atoms [39]. The binding of noble gas atoms to CUO causes a changeover in the electronic ground state of the resulting CUO(Ng)$_n$ complexes [40, 41]. Subsequent studies show that other actinide compounds such as UO$_2$ and UO$_2^+$ trapped in noble gas matrices are also coordinated by multiple noble gas atoms [42, 43]. We have performed a systematic matrix isolation infrared spectroscopic study and theoretical investigation of transition metal oxides trapped in solid noble gas matrices. Matrix isolation plays a very important role in providing valuable spectral and structural properties of transition metal oxides. Both transition metal oxide cations and neutral species with different oxidation states are considered. The results show that some transition metal oxide cations as well as neutral species trapped in solid noble gas matrices are not "isolated" species, but are chemically coordinated by one or multiple noble gas atoms. The criterion to judge what kind of species trapped in solid noble gas matrices

may become coordinated by noble gas atoms is given. The nature of the bonding and the relationship between vibrational frequency shifts and noble gas coordination are also discussed.

2 Experimental and theoretical methods

The experiments were performed by using pulsed laser evaporation–matrix isolation infrared absorption spectroscopy. Transition metal oxide molecules were generated either via reactions of laser-evaporated metal atoms with dioxygen or by laser evaporation of bulk metal oxide targets. The metal dioxides and higher oxide molecules were prepared via reactions between metal atoms and dioxygen, while the metal monoxide molecules were produced via laser evaporation of bulk metal oxide targets. Most transition metals exhibit several oxidation states, and hence, the species evaporated from the bulk metal oxide target usually are a mixture of oxides with different oxidation states. For some transition metals, we were able to prepare relatively 'pure' transition metal monoxides by laser ablation of selected metal oxide targets with controlled laser energies.

The experimental apparatus for pulsed laser evaporation–matrix isolation infrared spectroscopy has been described in detail elsewhere [3, 5]. Briefly, the 1064 nm Nd:YAG laser fundamental (Spectra Physics, DCR 150, 20 Hz repetition rate and 8 ns pulse width) was focused onto a rotating bulk metal or metal oxide target. The laser evaporated metal atoms or metal oxide species were co-deposited with reagent gas in excess noble gases onto a cryogenic window, which was maintained at 6–10 K by means of a closed-cycle helium refrigerator. The samples were usually deposited for one to two hours. Because of the very low temperature of the deposit, the laser-evaporated species were quenched to their ground state in solid matrices. The as-deposited samples were annealed to higher temperatures to allow trapped reactants to diffuse and to react. The infrared absorption spectra of the products in the mid-infrared region (4000–400 cm^{-1}) were recorded on a Bruker IFS 66v/s spectrometer at 0.5 cm^{-1} resolution using a deuterated triglycine sulfate (DTGS) or liquid nitrogen cooled HgCdTe (MCT) detector. As a structure-specific spectroscopic technique, infrared absorption spectroscopy is a sensitive method for detecting transition metal oxides in solid matrices. Metal oxide molecules often exhibit strong absorptions in the terminal M=O and bridging M–O–M stretching vibrational regions. Isotopic substitution experiments are extremely important for product identification and structural determination. Isotopically-labeled ^{18}O$_2$ samples were used in our transition metal and dioxygen reaction experiments. The experimentally observed oxygen isotopic shifts give information about the extent of oxygen atom(s) participation in the observed vibrational modes. The use of isotopic ^{16}O$_2$ + ^{18}O$_2$ and ^{16}O$_2$ + ^{16}O^{18}O + ^{18}O$_2$ mixtures results in mul-

tiple absorptions for different isotopomers, which is a major factor in determining the number of oxygen atoms involved in the observed vibrational modes.

In order to determine whether or not the trapped species are coordinated by noble gas atoms and, if so, to determine the number of coordinated noble gas atoms, we used mixtures of a lighter noble gas host doped with heavier noble gas atoms as a matrix. If the trapped species are coordinated by noble gas atoms, the coordinated lighter noble gas atoms can be successively substituted by heavier noble gas atoms when annealing the solid matrix sample, which will induce vibrational frequency shifts in the infrared spectrum. The coordination number can be determined by the number of new absorption bands formed.

Quantum chemical calculations were performed in order to predict molecular properties including equilibrium geometries, energies and vibrational frequencies of noble gas–transition metal oxide complexes. The evaluation of accurate molecular properties and energies usually needs sophisticated high level *ab initio* calculations. However, it is very difficult to carry out calculations on transition metal-containing systems with high level *ab initio* methods. Density functional theory (DFT) has the advantage of predicting equilibrium geometries and vibrational frequencies that are comparable in quality to those obtained with more highly correlated methods for transition metal-containing compounds [44, 45]. Well-calibrated DFT methods [46–48] such as B3LYP as well as the second-order Møller-Plesset perturbation (MP2) method were utilized in this study. The $6\text{-}311+G(d)$, $6\text{-}311+G(3df)$ basis set was used for the O, Ar, Kr and first row transition metal atoms [49–51]. The SDD pseudopotential and basis sets were used for the third row transition metals [52, 53]. The DGDZVP basis sets were used for the Xe and second row transition metal atoms [54, 55]. Geometries were fully optimized, and the stability of the electronic wave function was tested; the harmonic vibrational frequencies were calculated using the analytic second derivatives, and zero-point energies (ZPE) were derived. The single-point energies of selected structures optimized at the B3LYP level were calculated using the CCSD(T) method [56]. All calculations were performed using the Gaussian 03 program [57].

3   Noble gas–transition metal oxide complexes

3.1   Transition metal monoxide cationic complexes

As the first transition metal in the series, scandium possesses the simplest electronic structure with only three valence electrons, and ScO^+ is the simplest transition metal oxide cation. The ScO^+ cation can be produced by pulsed laser ablation of a bulk Sc_2O_3 target. As shown in Figure 1, co-deposition of laser-evaporated scandium oxides with pure argon or krypton at 12 K forms ScO as the major product with minor absorptions from ScO^+ and ScO_2^-; these
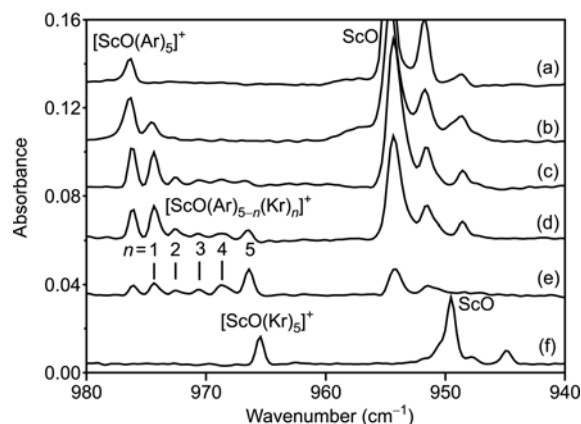

Figure 1   Infrared spectra in a selected region from co-deposition of laser-evaporated scandium oxides with noble gases. (a) Pure argon, after sample deposition at 12 K, (b) 3% krypton in argon, after deposition at 12 K, (c) after annealing (b) to 35 K, (d) after annealing (b) to 40 K, (e) after annealing (b) to 45 K, and (f) pure krypton, after sample deposition at 12 K.

were previously identified on the basis of the effects of isotopic substitution in their infrared spectra and by theoretical calculations [58, 59]. When the argon matrix was doped by 3% krypton, five new absorptions appeared upon annealing the sample to different temperatures. These absorptions lay between the ScO^+ absorptions in pure argon and in pure krypton. When the matrix sample was annealed to higher temperatures step by step, the intensities of the more red-shifted bands increased, whereas those of the higher frequency bands in the progression decreased. The intervals between the neighboring absorptions were almost equal. A similar five-band progression with almost equivalent intervals was also observed in an experiment where xenon was doped into krypton. These experimental observations suggest that ScO^+ is coordinated by multiple noble gas atoms in solid noble gas matrices and the observation of five distinct new absorptions in doped experiments strongly suggests that five noble gas atoms are coordinated to ScO^+ in the inner sphere. Hence, the absorption previously assigned to isolated ScO^+ in solid argon should be reassigned to the $[ScO(Ar)_5]^+$ complex isolated in solid argon, and the new bands in the mixed matrix experiments assigned to the mixed complexes [60].

Consistent with the experimental observations, density functional theoretical calculations indicated that ScO^+ is able to coordinate five noble gas atoms in the first coordination sphere [60]. The calculation results show that the maximum total binding energy for the $[ScO(Ng)_n]^+$ complexes (Ng = Ar, Kr, or Xe) is achieved with $n = 5$. When $n = 6$, the magnitude of the binding energy decreases, which indicates that binding the sixth noble gas atom is repulsive. The $[ScO(Ng)_5]^+$ complexes are predicted to have C_{4v} symmetry with one axial noble gas atom and four equivalent equatorial noble gas atoms (Figure 2). The calculations also show that upon successive replacement of Ar atoms by Kr
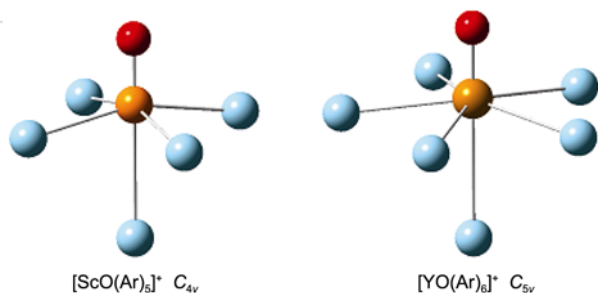
Figure 2 Optimized structures for the [ScO(Ar)$_5$]$^+$ and [YO(Ar)$_6$]$^+$ complexes.

atoms, or on replacing Kr atoms by Xe atoms, the total binding energy increases, whereas the Sc–O stretching frequency red-shifts monotonically.

In experiments where laser-evaporated yttrium oxides were co-deposited with krypton doped into argon, six new bands lying between the YO$^+$ absorption in pure argon and that in pure krypton evolved on annealing. This suggests that the YO$^+$ cation is coordinated by six noble gas atoms in both solid argon and solid krypton. In the experiment with xenon doped into argon, five new absorptions were observed, which suggests that the YO$^+$ cation can only coordinate five xenon atoms. Consistent with the experimental observations, density functional theoretical calculations indicated that YO$^+$ can coordinate six argon or krypton atoms, but only five xenon atoms. The [YO(Ar)$_6$]$^+$ complex has C_{5v} symmetry (Figure 2) [61].

3.2 Neutral 3d transition metal monoxide complexes

The spectra, electronic structure and bonding of 3d transition metal monoxides have been the subject of intensive experimental and theoretical investigations. Their ground spin states and vibrational frequencies in the gas phase and in solid noble gas matrices have been reliably established [62–68]. In general, the matrix frequencies are usually slightly red-shifted from the gas phase values with the shift in the argon matrix being larger than that for neon. Experiments were performed on the neutral first row transition metal monoxide species in solid noble gas matrices [69]. It was found that the late transition metal monoxides, from CrO to NiO, were coordinated by one noble gas atom forming noble gas–transition metal monoxide complexes in solid noble gas matrices. Figure 3 shows the spectra of chromium monoxide in doped experiments, which clearly show that only one noble gas atom is coordinated to CrO. Theoretical calculations indicate that the ground states of (Ng)CrO, (Ng)MnO, (Ng)FeO, (Ng)CoO, and (Ng)NiO complexes are linear, and correlate with the ground states of the metal monoxides. In contrast to the late transition metal monoxides, the early transition metal monoxide molecules, ScO, TiO and VO, do not form noble gas complexes in solid noble gas matrices. Consistent with the experimental observations, quantum chemical calculations on ArScO, ArTiO, and
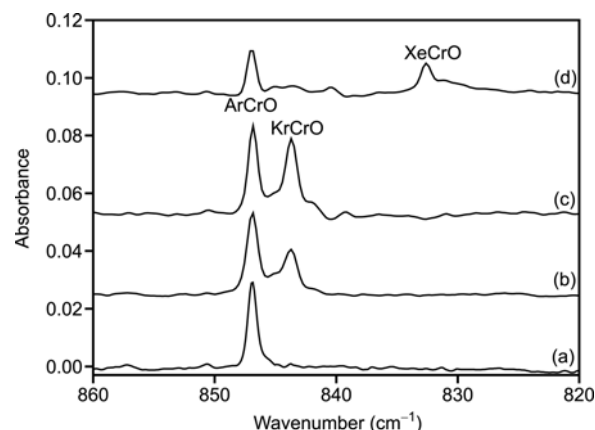

Figure 3 Infrared spectra in a selected region from co-deposition of laser-evaporated chromium monoxide with noble gases. (a) Pure Ar, after sample deposition at 6 K followed by annealing to 25 K, (b) 2% Kr in Ar, after sample deposition at 6 K, (c) after annealing of (b) to 25 K, and (d) 1% Xe in Ar, after sample deposition at 6 K followed by annealing to 25 K.

ArVO almost converge to separated MO and Ar (with the M–Ar distances larger than 6 Å) with negligible binding energies, which indicates that ScO, TiO, and VO cannot form complexes with Ar.

3.3 Higher transition metal oxide complexes

Higher oxide species are also able to form a variety of noble gas complexes [70–73]. Experiments were performed on group VB metal dioxide and tetroxide molecules [70, 71]. The spectra in the V=O stretching frequency region for the product of co-deposition of laser-evaporated vanadium atoms with dioxygen in excess argon doped with xenon are shown in Figure 4. The spectra clearly show that VO$_2$ coordinates two Ar or Xe atoms and that VO$_4$ coordinates one Ar or Xe atom in solid noble gas matrixes. Hence, the VO$_2$
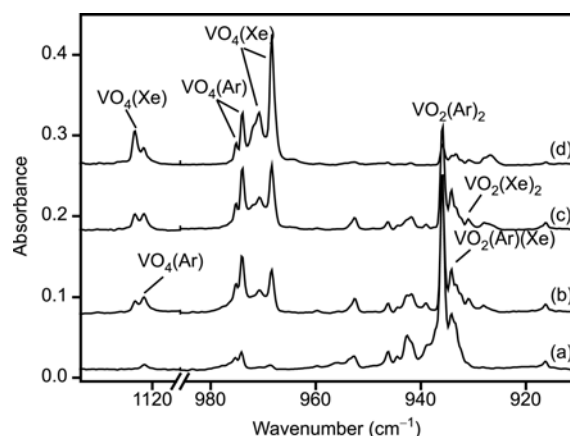

Figure 4 Infrared spectra in the selected regions from co-deposition of laser-ablated vanadium atoms with 1% O$_2$ + 1% Xe in argon. (a) Sample deposition for 1 h at 12 K, (b) after annealing to 35 K, (c) after annealing to 40 K, and (d) after annealing to 45 K.

and VO$_4$ molecules trapped in solid noble gas matrixes should be regarded as VO$_2$(Ng)$_2$ and VO$_4$(Ng) (Ng = Ar or Xe) complexes. The VO$_2$(Ng)$_2$ complex is predicted to have a $^2A_1$ ground state with C_{2v} symmetry. The V–O bond length is elongated upon noble gas atom coordination with both the symmetric and antisymmetric V–O stretching vibrational frequencies being red-shifted.

The VO$_4$ molecule was shown to be a vanadium dioxide-dioxygen complex with vanadium in its highest +V oxidation state, and predicted to have a $^2A_2$ ground state with C_{2v} symmetry (Figure 5) [70]. Doping experiments suggested that the VO$_4$ molecule is coordinated by one noble gas atom forming a VO$_4$(Ng) complex in solid noble gas matrices, and thus is predicted to have a $^2A''$ ground state with C_s symmetry (Figure 5). The noble gas atom and the coordinated O$_2$ subunits are in the same plane and perpendicular to the VO$_2$ plane. The two O atoms in the O$_2$ fragment are slightly inequivalent due to noble gas atom coordination. Therefore, the O–O stretching mode should be split into four bands with two closely-spaced intermediate absorptions in the mixed $^{16}O_2 + ^{16}O^{18}O + ^{18}O_2$ spectrum; this is consistent with the experimental observations [74].

Recent investigations of oxygen-rich chromium oxide species provide a good illustration that noble gas atoms can not only form direct chemical bonds with metals but also participate in chemical reactions in a noble gas matrix and induce a remarkable disproportionation reaction [72]. Laser-evaporated chromium atoms were shown to insert into dioxygen to form CrO$_2$ in solid argon [75]. Annealing allowed diffusion and reaction to form a (η^2–O$_2$)$_2$CrO$_2$ complex [72, 76]. The complex is predicted to have a $^3B_2$ ground state with a tetrahedral skeleton of C_{2v} symmetry, in which the two O$_2$ fragments lie in the same plane, perpendicular to the OCrO plane. The two η^2–O$_2$ fragments are
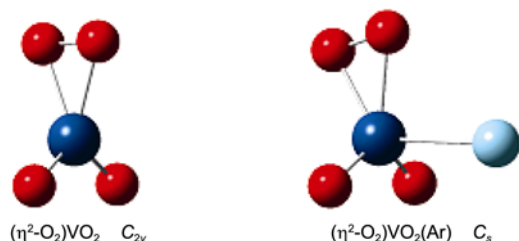

Figure 5   Optimized structures of the VO$_4$ and VO$_4$(Ar) complexes.

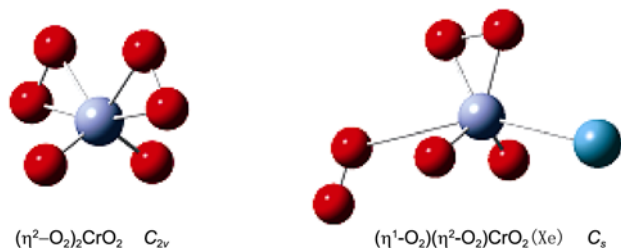**Figure 6**   Optimized structures of the CrO$_6$ and CrO$_6$(Xe) complexes.

equivalent, and bound in an asymmetric, side-on fashion, with two inequivalent Cr–O bond lengths (Figure 6). This complex was shown to be [(O$_2^-$)$_2$(CrO$_2$)$^{2+}$], a side-on bonded disuperoxo–chromium dioxide complex with chromium in its highest +VI oxidation state. It was found that the (η^2–O$_2$)$_2$CrO$_2$ complex further reacts with xenon atoms doped in solid argon to give (η^1–OO)(η^2–O$_2$)CrO$_2$(Xe), which is predicted to have C_s symmetry and a $^3A''$ ground state with the two O$_2$ fragments and the xenon atom in the same plane, perpendicular to the OCrO plane (Figure 6). The end-on bonded η^1–OO fragment is predicted to have an O–O bond length of about the same as that in free O$_2$. The complex can be regarded as an triplet O$_2$ molecule adsorbed on a closed-shell (η^2–O$_2$)CrO$_2$(Xe) complex. The calculated O–O distance in the latter (η^2–O$_2$)CrO$_2$(Xe) fragment is typical of that of a peroxide ligand. Therefore, the (η^2–O$_2$)CrO$_2$(Xe) fragment can be characterized as a side-on bonded peroxo-chromium dioxide–xenon complex. The Cr–Xe bond has a theoretically optimized bond distance of 2.892 Å and a binding energy of 14.0 kcal/mol with respect to the (O$_2$)CrO$_2$ ($^1A_1$) + Xe asymptotes at the CCSD(T)// B3LYP level after zero-point energy correction [72].

4   Bonding mechanism

The experimental observations indicate that although some transition metal oxides are able to coordinate one or multiple noble gas atoms, other transition metal oxides are not able to do so. In the above-characterized noble gas–transition metal oxide complexes, the interactions between noble gas atoms and transition metal oxides involve ion–induced dipole interactions as well as chemical bonding interactions. The noble gas atoms act as an electron donor (ligand), and the bonding involves the donation of a lone pair from the noble gas atoms into empty, primarily metal-based, orbitals. According to molecular orbital theory, the bonding efficiency between fragment orbitals is determined by three main factors: symmetry matching, extent of overlap and energy similarity. Based upon these three requirements, the experimental observations can be satisfactorily explained as follows.

The ScO$^+$ cation has a $^1\Sigma^+$ ground state with an electronic configuration of $(8\sigma)^2$ $(3\pi)^4$ $(9\sigma)^0$ $(1\delta)^0$. The 9σ LUMO is primarily a nonbonding hybrid of the Sc 4s and 3dz^2 orbitals that is directed away from the O atom. The 1δ LUMO+1 molecular orbital is largely the Sc 3d orbital that is mainly nonbonding. These orbitals are the primary acceptor orbitals for donation from noble gas atoms. It is found that the HOMO-14 (6b$_2$) and HOMO-17 (17a$_1$) in [ScO(Ar)$_5$]$^+$ shown in Figure 7 are bonding orbitals that involve donation from the filled Ar 3p orbitals into the empty 9σ and 1δ orbitals of ScO$^+$. The YO$^+$ cation has a similar electronic configuration to that of ScO$^+$. According to the calculation
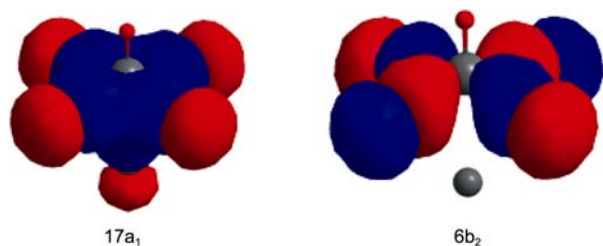
Figure 7   The bonding molecular orbitals of [ScO(Ar)$_5$]$^+$.

results, the yttrium-based nonbonding σ LUMO of YO$^+$ is at virtually the same energy level as the 9σ LUMO of ScO$^+$, but the energy level of the LUMO + 1 yttrium-based non-bonding δ orbital is about 0.7 eV higher in energy than that of the 1δ LUMO+1 orbital of ScO$^+$. Hence, donation from the filled Ar 3p orbitals into the LUMO of YO$^+$ dominates the bonding interaction in the [YO(Ar)$_6$]$^+$ and [YO(Kr)$_6$]$^+$ complexes.

The early transition metal monoxide neutrals, ScO, TiO and VO do not form stable noble gas complexes. The LU-MOs of these neutral species lie much higher in energy than the corresponding orbitals of the cations, and thus the above-mentioned donation interactions are not observed. For the late transition metal monoxide neutral species, the valence orbitals involved in bonding lie much lower in energy than the valence orbitals of the early transition metal monoxides, as shown in Figure 8. Therefore, the late transition metal monoxide neutral species are able to form weakly bound noble gas complexes. The orbital energies decrease from CrO to NiO, and therefore, the binding energies of the noble gas–transition metal monoxide complexes increase from CrO to NiO, as shown in Figure 9. Mulliken charge population analysis shows that the noble gas atoms are positively charged, and that the charge density increases from Ar to Kr to Xe, and from Cr to Ni. Similarly, the group VB metal dioxides are able to coordinate two noble gas atoms to
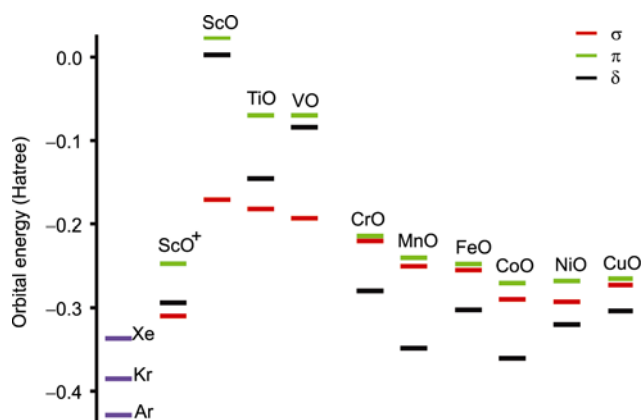

Figure 8   Calculated relative energies of the valence molecular orbitals of first row transition metal monoxide cations and neutral species, and the outermost p orbitals of noble gas atoms.
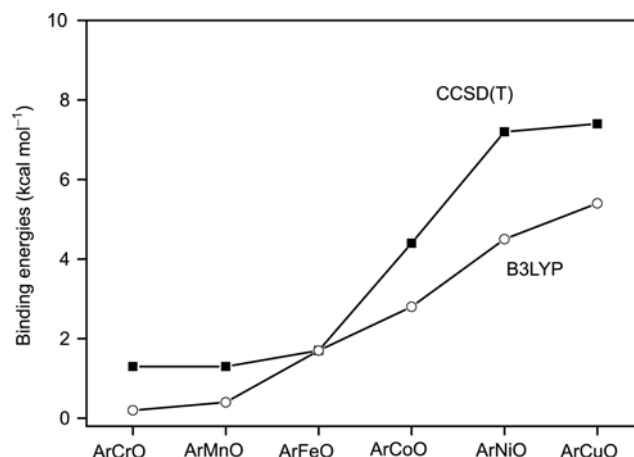

Figure 9   Binding energies of the ArMO complexes calculated at the B3LYP and CCSD(T)//B3LYP levels of theory.

form the MO$_2$(Ng)$_2$ (M = V, Nb, Ta, Ng = Ar, Kr and Xe) complexes, while the MO$_4$ molecules only coordinate one noble gas atom in forming the MO$_4$(Ng) complexes (Ng = Ar, Kr, Xe for M = V, Nb and Ta, and Ng = Xe for M = Cr).

On the basis of the bonding analysis, some common trends can be drawn: (1) In these noble gas–transition metal oxide complexes, the noble gas atoms act as a ligand, and are coordinated to the metal center of the transition metal oxides, which is positively charged (electrophilic); (2) the molecular orbitals of the metal oxides that are involved in bonding are localized metal-based orbitals; (3) only the transition metal oxides which have low-lying unoccupied or partially occupied MOs are able to coordinate noble gas atom(s) and form noble gas complexes.

The M–Ng binding energies for the above-characterized noble gas–transition metal oxide complexes calculated at the B3LYP and CCSD(T)//B3LYP levels of theory are listed in Table 1. The values calculated at the B3LYP level are systematically smaller than those calculated at the CCSD(T) level because of the lack of proper treatment of dispersive interactions with B3LYP. These values are comparable to those measured for transition metal carbonyl–noble gas complexes [17]. The calculated M–Ng binding energies increase when Ar is replaced by Kr and Xe. The increasing binding energies from Ar to Xe are consistent with the experimental observations that heavier noble gas atoms can readily replace lighter noble gas atoms in the (Ng)MO complexes. The binding energies of the (Ng)MO complexes increase in the order CrO < MnO < FeO < CoO < NiO. The binding energies of the metal monoxide cations are higher than those of the corresponding neutral monoxide species. In general, the binding energies also increase with increasing oxidation state of the metal center.

The experimentally observed vibrational frequency differences between the transition metal monoxides in the gas phase and the noble gas–metal monoxide complexes in a solid argon matrix, together with the frequency shifts when

Table 1 Calculated binding energies (kcal/mol) per noble gas atom (Ng) of the noble gas–transition metal oxide complexes at the B3LYP and CCSD(T)//B3LYP (in parentheses) levels of theory

Complex	Ng = Ar	Ng = Kr	Ng = Xe
$[ScO(Ng)_5]^+$	4.4	6.4	7.7
$[YO(Ng)_6]^+$	3.1	4.4	7.3 [a]
$(Ng)CrO$	0.2 (1.3)	0.9 (2.1)	2.3 (3.1)
$(Ng)MnO$	0.4 (1.3)	1.1 (2.2)	2.0 (4.5)
$(Ng)FeO$	1.7 (1.7)	2.8 (2.9)	4.1 (6.0)
$(Ng)CoO$	2.8 (4.4)	4.1 (6.5)	5.7 (10.1)
$(Ng)NiO$	4.5 (7.2)	6.0 (9.2)	7.6 (13.1)
$VO_2(Ng)_2$	6.3 (12.8)		12.7(18.2)
$NbO_2(Ng)_2$	3.6(6.8)	5.6(8.8)	7.0(9.0)
$VO_4(Ng)$	0.8 (5.0)		3.8 (7.3)
$NbO_4(Ng)$	4.2(3.9)	5.4(5.3)	6.0(6.9)
$TaO_4(Ng)$	6.9 (7.5)	8.6 (9.3)	11.4 (10.6)
$(\eta^2-O_2)CrO_2(Ng)$			(14.0)

a) The binding energy of the $[YO(Xe)_5]^+$ complex.

Table 2 Experimentally observed vibrational frequency differences (cm^{-1}) between MO in the gas phase and (Ng)MO in a solid argon matrix (Gas-Ar), and the frequency shifts when the coordinated argon atom(s) is replaced by Kr (Ar–Kr) or Xe (Ar–Xe) for the noble gas–transition metal oxide complexes in solid argon

	Mode	Gas-Ar	Ar-Kr	Ar-Xe
$[ScO(Ng)_5]^+$	Sc = O str.		−9.8	
$[YO(Ng)_6]^+$	Y = O str.		−7.7	−24.1
$(Ng)CrO$	Cr = O str.	−38.7	−2.5	−13.7
$(Ng)MnO$	Mn = O str.	+0.7	+3.7	+7.4
$(Ng)FeO$	Fe = O str.	+1.6	+1.8	+3.5
$(Ng)CoO$	Co = O str.	−5.5	−1.1	−4.2
$(Ng)NiO$	Ni = O str.	−2.6	−1.7	−4.5
$VO_2(Ng)_2$	sym. OVO str.			−1.7
	antisym. OVO str.			−4.9
	O-O str.			+2.1
$VO_4(Ng)$	sym. OVO str.			−6.4
	antisym. OVO str.			−9.0

the coordinated Ar atom(s) is replaced by Kr or Xe for the above-mentioned noble gas–transition metal oxide complexes in solid argon are listed in Table 2. For the noble gas complexes investigated, the observed vibrational frequencies of some species are red-shifted when the coordinated Ar atom(s) is replaced by Kr or Xe, while some others are blue-shifted. Furthermore, for a given complex, the shifts for different vibrational modes may not be the same. Taking the VO$_4$(Ar) complex as an example, when the coordinated Ar atom is replaced by Kr or Xe, the V = O stretching modes are red-shifted whereas the O–O stretching mode is blue- shifted. It was found that the frequency shifts have no direct relationship with the calculated binding energies. In general, the frequency shifts depend mainly on the nature of the molecular orbitals that are involved in bonding. If the electron density of the noble gas atom is donated into a bonding orbital of the transition metal oxide fragment, the corresponding vibration will be blue-shifted, whereas if an antibonding orbital is involved, the corresponding vibration will be red-shifted; no obvious frequency shift is expected if

only a nonbonding orbital is involved.

5   Conclusions

A combined matrix isolation infrared spectroscopic study and theoretical investigation of transition metal oxide molecules trapped in solid noble gas matrices indicates that some transition metal oxide species trapped in solid noble gas matrices become chemically coordinated by one or multiple noble gas atoms and form noble gas complexes, and hence, they cannot be regarded as isolated species.

Bonding analysis shows that the interactions between noble gas atoms and transition metal oxides involve ion-induced dipole interactions as well as chemical bonding interactions. The noble gas atoms act as an electron donor (ligand), and the bonding involves the donation of a lone pair of the noble gas atoms into empty, primarily metal-based orbitals. The results suggest that if the transition metal species trapped in a solid noble gas matrix has an electrophilic center with localized low lying unoccupied or partially occupied molecular orbitals, it is able to coordinate noble gas atom(s) and form noble gas–transition metal complexes. The coordination of noble gas atoms leads to a shift of the vibrational frequencies of the transition metal species. The observed frequency shifts largely depend on the nature of the valence orbitals involved in bonding. There is no direct correlation between the matrix shifts and the strength of noble gas coordination.

1   Whittle E, Dows DA, Pimentel GC. Matrix isolation method for the experimental study of unstable species. *J Chem Phys*, 1954, 22: 1943

2   Bondybey VE, Smith AM, Agreiter J. New developments in matrix isolation spectroscopy. *Chem Rev*, 1996, 96: 2113–2134

3   Zhou MF, Andrews L, Bauschlicher CWJr. Spectroscopic and theoretical investigations of vibrational frequencies in binary unsaturated transition-metal carbonyl cations, neutrals, and anions. *Chem Rev*, 2001, 101: 1931–1961

4   Himmel HJ, Downs AJ, Greene TM. Reactions of ground state and electronically excited atoms of main group elements: A matrix perspective. *Chem Rev*, 2002, 102: 4191–4241

5   Wang GJ, Zhou MF. Probing the intermediates in the $MO + CH_4 \leftrightarrow M + CH_3OH$ reactions by matrix isolation infrared spectroscopy. *Int Rev Phys Chem*, 2008, 27: 1–25

6   Jacox ME. The vibrational energy levels of small transient molecules isolated in neon and argon matrices. *Chem Phys*, 1994, 189: 149–170

7   Jacox ME. The spectroscopy of molecular reaction intermediates trapped in the solid rare gases. *Chem Soc Rev*, 2002, 31: 108–115

8   Bartlett N. Xenon hexafluoroplatinate(V) $Xe^+[PtF_6]^-$. *Proc Chem Soc*, 1962: 218

9   Turner JJ, Pimentel GC. Krypton fluoride, preparation by the matrix isolation technique. *Science*, 1963, 140: 974–975

10   Khriachtchev L, Räsänen M, Gerber RB. Noble-gas hydrides: New chemistry at low temperatures. *Acc Chem Res*, 2009, 42: 183–191

11   Khriachtchev L, Pettersson M, Runeberg N, Lundell J, Räsänen M. A stable argon compound. *Nature*, 2000, 406: 874–876

12   Perutz RN, Turner JJ. Photochemistry of the group 6 hexacarbonyls in low-temperature matrices, III. Interaction of the pentacarbonyls with noble gases and other matrices. *J Am Chem Soc*, 1975, 97: 4791–4800

13   Burdett JK, Grzybowsky JM, Perutz RN, Poliakoff M, Turner JJ, Turner R F. Photolysis and spectroscopy with polarized light, key to the photochemistry of $Cr(CO)_5$ and related species. *Inorg Chem*, 1978, 17: 147–154

14   Turner JJ, Burdett JK, Perutz RN, Poliakoff M. Matrix photochemistry of metal carbonyl. *Pure Appl Chem*, 1977, 49: 271–285

15   Simpson MB, Poliakoff M, Turner JJ, Maier WB, McLaughlin JG. $[Cr(CO)_5Xe]$ in solution, the first spectroscopic evidence. *J Chem Soc Chem Commun*, 1983: 1355–1357

16   Sun X, George MW, Kazarian SG, Nikiforov SM, Poliakoff M. Can organometallic noble gas compounds be observed in solution at room temperature? A time-resolved infrared (TRIR) and UV spectroscopic study of the photochemistry of $M(CO)_6$ (M = Cr, Mo, and W) in supercritical noble gas and CO_2 solution. *J Am Chem Soc*, 1996, 118: 10525–10532

17   Wells JR, Weitz E. Rare gas–metal carbonyl complexes, bonding of rare gas atoms to the group VI pentacarbonyls. *J Am Chem Soc*, 1992, 114: 2783–2787

18   Portius P, Yang JX, Sun X, Grills DC, Matousek P, Parker AW, Towrie M, George MW. Unraveling the photochemistry of $Fe(CO)_5$ in solution, observation of $Fe(CO)_3$ and the conversion between $^3Fe(CO)_4$ and $^1Fe(CO)_4$(solvent). *J Am Chem Soc*, 2004, 126: 10713–10720

19   Grills DC, Sun XZ, Childs GI, George MW. An investigation into the reactivity of organometallic noble gas complexes: A time-resolved infrared study in supercritical noble gas and alkane solution at room temperature. *J Phys Chem A*, 2000, 104: 4300–4307

20   Grills DC, Childs GI, George MW. The characterization and reactivity of $(\eta^5\text{-}C_5H_5)M(CO)_3(Xe)$ (M = Nb or Ta) in solution at room temperature. *Chem Commun*, 2000, 1841–1842

21   Weiller BH, Wasserman EP, Bergman RG, Moore CB, Pimentel GC. Time-resolved IR spectroscopy in liquid rare gases, direct rate measurement of an intermolecular alkane carbon–hydrogen oxidative addition reaction. *J Am Chem Soc*, 1989, 111: 8288–8290

22   Schultz RH, Bengali AA, Tauber MJ, Weiller BH, Wasserman EP, Kyle KR, Moore CB, Bergman RG. IR flash kinetic spectroscopy of C–H bond activation of cyclohexane-d0 and d12 by $Cp^*Rh(CO)_2$ in liquid rare gases, kinetics, thermodynamics, and unusual isotope effect. *J Am Chem Soc*, 1994, 116: 7369–7377

23   Jina OS, Sun XZ, George MW. Do early and late transition metal noble gas complexes react by different mechanisms? A room temperature time-resolved infrared study of $(\eta^5\text{-}C_5R_5)Rh(CO)_2$ (R = H or Me) in supercritical noble gas solution at room temperature. *Dalton Trans*, 2003:1773–1778

24   Yeston JS, McNamara BK, Bergman RG, Moore CB. Flash infrared kinetics of the photochemistry of $Tp^*Rh(CO)_2$ and $Bp^*Rh(CO)_2$ in liquid xenon solution. *Organometallics*, 2000, 19: 3442–3446

25   Sun XZ, Grills DC, Nikiforov SM, Poliakoff M, George MW. Remarkable stability of $(\eta^5\text{-}C_5H_5)Re(CO)_2L$ (L = n-heptane, Xe, and Kr): A time-resolved infrared spectroscopic study of $(\eta^5\text{-}C_5H_5)Re(CO)_3$ in conventional and supercritical fluid solution. *J Am Chem Soc*, 1997, 119: 7521–7525

26   Ball GE, Darwish TA, Geftakis S, George MW, Lawer DJ, Portius P, Rourke J. Characterization of an organometallic xenon complex using NMR and IR spectroscopy $Re(^iPrCp)(CO)(PF_3)Xe$. *Proc Natl Acad Sci USA*, 2005, 120: 1853–1858

27   McMaser J, Portius P, Ball GE, Rourke JP, George MW. Density functional theoretical studies of the Re–Xe bonds in $Re(Cp)(CO)(PF_3)$-Xe and $Re(Cp)(CO)_2Xe$. *Organometallics*, 2006, 25, 5242–5248

28   Seidel S, Seppelt K. Xenon as a complex ligand: The tetra xenono gold(II) cation in $AuXe_4^{2+}(Sb_2F_{11}^-)_2$. *Science*, 2000, 290: 117–118

29   Seppelt KZ. Metal–xenon complexes. *Anorg Allg Chem*, 2003, 629: 2427–2430

30   Drews T, Seidel S, Seppelt K. Gold–xenon complexes. *Angew Chem Int Ed*, 2002, 41: 454–456

31   Hwang IC, Seidel S, Seppelt K. Gold(I) and mercury(II) xenon complexes. *Angew Chem Int Ed*, 2003, 42: 4392–4395

32   Evans CJ, Gerry MCL. The microwave spectra and structure of Ar–AgX (X = F, Cl, Br). *J Chem Phys*, 2000, 112: 1321–1329

33   Evans CJ, Gerry MCL. Noble gas–metal chemical bonding? The microwave spectra, structures, and hyperfine constants of Ar–CuX (X = F, Cl, Br). *J Chem Phys*, 2000, 112: 9363–9374

34   Evans CJ, Lesarri A, Gerry MCL. Noble gas–metal chemical bonds. Microwave spectra, geometries, and nuclear quadrupole coupling constants of Ar–AuCl and Kr–AuCl. *J Am Chem Soc*, 2000, 122: 6100–6105

35   Evans CJ, Rubinoff DS, Gerry MCL. Noble gas–metal chemical bonding: The microwave spectra, structures and hyperfine constants of Ar–AuF and Ar–AuBr. *Phys Chem Chem Phys*, 2000, 2: 3943–3948

36   Thomas JM, Walker NR, Cooke SA, Gerry MCL. Microwave spectra and structures of KrAuF, KrAgF, and KrAgBr; [83]Kr nuclear quadrupole coupling and the nature of noble gas–noble metal halide bonding. *J Am Chem Soc*, 2004, 126: 1235–1246

37   Cooke SA, Gerry MCL. Insights into the xenon–silver halide interaction from a rotational spectroscopic study of XeAgF and XeAgCl. *Phys Chem Chem Phys*, 2004, 6: 3248–3256

38   Cooke SA, Gerry MCL. XeAuF. *J Am Chem Soc*, 2004, 126: 17000–17008

39   Li J, Bursten BE, Liang BY, Andrews L. Noble gas–actinide compounds: Complexation of the CUO molecule by Ar, Kr, and Xe atoms in noble gas matrices. *Science*, 2002, 295: 2242–2245

40   Andrews L, Liang BY, Li J, Bursten BE. Noble gas–actinide complexes of the CUO molecule with multiple Ar, Kr, and Xe atoms in noble-gas matrices. *J Am Chem Soc*, 2003, 125: 3126–3139

41   Andrews L, Liang BY, Li J, Bursten BE. Ground-state reversal by matrix interaction, electronic states and vibrational frequencies of CUO in solid argon and neon. *Angew Chem Int Ed*, 2000, 39: 4565–4567

42   Li J, Bursten BE, Andrews L, Marsden CJ. On the electronic structure of molecular UO_2 in the presence of Ar atoms: Evidence for direct U–Ar bonding. *J Am Chem Soc*, 2004, 126: 3424–3425

43   Wang XF, Andrews L, Li J, Bursten BE. Significant interactions between uranium and noble-gas atoms: Coordination of the UO_2^+ cation by Ne, Ar, Kr, and Xe atoms. *Angew Chem Int Ed*, 2004, 43: 2554–2557

44   Sousa SF, Fernandes PA, Ramos MJ. General performance of density functionals. *J Phys Chem A*, 2007, 111: 10439–10452

45   Zhao Y, Truhlar DG.. Density functionals with broad applicability in chemistry. *Acc Chem Res*, 2008, 41: 157–167

46   Becke AD. Density-functional thermochemistry III. The role of exact exchange. *J Chem Phys*, 1993, 98: 5648–5652

47   Lee C, Yang W, Parr RG. Development of the Colle–Salvetti correlation-energy formula into a functional of the electron density. *Phys Rev B*, 1988, 37(2): 785–789

48   Møller C, Plesset MS. Note on an approximation treatment for many-electron systems. *Phys Rev B*, 1984, 46: 618–622

49   Wachter AJH. Gaussian basis set for molecular wavefunctions containing third-row atoms. *J Chem Phys*, 1970, 52: 1033–1036

50   Hay PJ. Gaussian basis sets for molecular calculations. The representation of 3d orbitals in transition-metal atoms. *J Chem Phys*, 1977, 66: 4377–4384

51   Raghavachari K, Trucks G W. Highly correlated systems. Excitation energies of first row transition metals Sc–Cu. *J Chem Phys*, 1989, 91: 1062–1065

52   Krishnan R, Binkley JS, Seeger R, Pople JA. Self-consistent molecular orbital methods. XX. A basis set for correlated wave functions. *J Chem Phys*, 1980, 72: 650–654

53   Andrae D, Haussermann U, Dolg M, Stoll H, Preuss H. Energy-adjusted *ab initio* pseudopotentials for the second and third row transition elements. *Theor Chim Acta*, 1990, 77: 123–141

54   McLean AD, Chandler GS. Contracted Gaussian basis sets for molecular calculations. I. Second row atoms, Z = 11–18. *J Chem Phys*, 1980, 72: 5639–5648

55   Sosa C, Andzelm J, Elkin BC, Wimmer E, Dobbs KD, Dixon DA. A local density functional study of the structure and vibrational frequencies of molecular transition-metal compounds. *J Phys Chem*, 1992, 96: 6630–6636

56   Pople JA, Gordon MH, Raghavachari K. Quadratic configuration interaction. A general technique for determining electron correlation energies. *J Chem Phys*, 1987, 87: 5968–5975

57   Gaussian 03, Revision B.05, Frisch MJ, Trucks GW, Schlegel HB, Scuseria GE, Robb MA, Cheeseman JR, Montgomery JAJr, Vreven T, Kudin KN, Burant JC, Millam JM, Iyengar SS, Tomasi J, Barone V, Mennucci B, Cossi M, Scalmani G, Rega N, Petersson GA, Nakatsuji H, Hada M, Ehara M, Toyota K, Fukuda R, Hasegawa J, Ishida M, Nakajima T, Honda Y, Kitao O, Nakai H, Klene M, Li X, Knox JE, Hratchian HP, Cross JB, Adamo C, Jaramillo J, Gomperts R, Stratmann RE, Yazyev O, Austin AJ, Cammi R, Pomelli C, Ochterski JW, Ayala PY, Morokuma K, Voth GA, Salvador P, Dannenberg JJ, Zakrzewski VG, Dapprich S, Daniels AD, Strain MC, Farkas O, Malick DK, Rabuck AD, Raghavachari K, Foresman JB, Ortiz JV, Cui Q, Baboul AG, Clifford S, Cioslowski J, Stefanov BB, Liu G, Liashenko A, Piskorz P, Komaromi I, Martin RL, Fox DJ, Keith T, Al-Laham M A, Peng CY, Nanayakkara A, Challacombe M, Gill PMW, Johnson B, Chen W, Wong MW, Gonzalez C, Pople JA. Gaussian, Inc., Pittsburgh, PA, 2003

58   Chertihin GV, Andrews L, Rosi M, Bauschlicher CWJr. Reactions of laser-ablated scandium atoms with dioxygen; Infrared spectra of ScO, OScO, $(O_2)ScO$, $(ScO)_2$, and $Sc(O_2)_2$. *J Phys Chem A*, 1997, 101: 9085–9091

59   Bauschlicher CWJr, Zhou MF, Andrews L, Johnson JRT, Panas I, Snis A, Roos BO. A further study of the products of scandium and dioxygen reactions. *J Phys Chem A*, 1999, 103: 5463–5467

60   Zhao YY, Wang GJ, Chen MH, Zhou MF. Noble gas–transition metal complexes: coordination of ScO^+ by multiple Ar, Kr and Xe atoms in noble gas matrices. *J Phys Chem A*, 2005, 109: 6621–6623

61   Zhao YY, Gong Y, Chen MH, Ding CF, Zhou MF. Coordination of ScO^+ and YO^+ by multiple Ar, Kr, and Xe atoms in noble gas matrixes: A matrix isolation infrared spectroscopic and theoretical study. *J Phys Chem A*, 2005, 109: 11765–11770

62   Merer AJ. Spectroscopy of the diatomic 3d transition metal oxides. *Annu Rev Phys Chem*, 1989, 40: 407–483

63   Huber KP, Herzberg G. *Constants of Diatomic Molecules*. New York: Van Nostrand-Reinhold, 1979

64   Harrison JF. Electronic structure of diatomic molecules composed of a first-row transition metal and main-group element (H–F). *Chem Rev*, 2000, 100: 679–716

65   Langhoff SR, Bauschlicher CWJr. *Ab initio* studies of transition metal systems. *Annu Rev Phys Chem*, 1988, 39: 181–212

66   Gutsev GL, Andrews L, Bauschlicher CWJr. Similarities and differences in the structure of 3d-metal monocarbides and monoxides. *Theor Chem Acc*, 2003, 109: 298–308

67   Bauschlicher CWJr, Maitre P. Theoretical study of the first transition row oxides and sulfides. *Theor Chim Acta*, 1995, 90: 189–203

68   Gong Y, Zhou MF, Andrews L. Spectroscopic and theoretical studies of transition metal oxides and dioxygen complexes. *Chem Rev*, 2009, 109: 6765–6808

69   Zhao YY, Gong Y, Zhou MF. Matrix isolation infrared spectroscopic and theoretical study of NgMO (Ng = Ar, Kr, Xe; M = Cr, Mn, Fe, Co, Ni) complexes. *J Phys Chem A*, 2006, 110: 10777–10782

70   Zhao YY, Gong Y, Chen MH, Zhou M F. Noble gas–transition-metal complexes: coordination of VO_2 and VO_4 by Ar and Xe atoms in solid noble gas matrixes. *J Phys Chem A*, 2006, 110: 1845–1849

71   Zhao YY, Zheng XM, Zhou MF. Coordination of niobium and tantalum oxides by Ar, Xe and O_2: Matrix isolation infrared spectroscopic and theoretical study of $NbO_2(Ng)_2$ (Ng = Ar, Xe) and $MO_4(X)$ (M = Nb, Ta; X=Ar, Xe, O_2) in solid argon. *Chem Phys*, 2008, 351, 13–18

72   Zhao YY, Su J, Gong Y, Li J, Zhou MF. Noble-gas-induced disproportionation reactions: facile superoxo-to-peroxo conversion on chromium dioxide. *J Phys Chem A*, 2008, 112: 8606–8611

73   Yang R, Gong Y, Zhou H, Zhou MF. Matrix isolation infrared spectroscopic and theoretical study of noble gas coordinated rhodium–dioxygen complexes. *J Phys Chem A*, 2007, 111: 64–70

74   Chertihin GV, Bare WD, Andrews L. Reactions of laser-ablated vanadium atoms with dioxygen. Infrared spectra of VO, VO_2, $OOVO_2$, and V_2O_2 in solid argon. *J Phys Chem A*, 1997, 101: 5090–5095

75   Chertihin GV, Bare WD, Andrews L. Reactions of laser-ablated chromium atoms with dioxygen. Infrared spectra of CrO, OCrO, CrOO, CrO_3, $Cr(OO)_2$, Cr_2O_2, Cr_2O_3 and Cr_2O_4 in solid argon. *J Chem Phys*, 1997, 107: 2798–2806

76   Zhou MF, Andrews L. Infrared spectra and density functional calculations of the CrO_2^-, MoO_2^-, and WO_2^- molecular anions in solid neon. *J Chem Phys*, 1999, 111: 4230–4238